Int. J. Heat Mass Transfer. Vol. 33, No. 9, pp. 1781–1793, 1990
Printed in Great Britain

0017-9310/90 $3.00+0.00

Application of a spherical thermal conductivity cell to solid n-eicosane paraffin

P. C. STRYKER
Department of Mechanical Engineering, Bucknell University, Lewisburg, PA 17837, U.S.A.

and

E. M. SPARROW
Department of Mechanical Engineering, University of Minnesota, Minneapolis, MN 55455, U.S.A.

(*Received* 1 *September* 1989 *and in final form* 9 *November* 1989)

Abstract—A precisely fabricated, spherical thermal conductivity cell is used to achieve steady, one-dimensional, loss-free radial heat conduction across an annular test specimen. The investigated test specimens are solid, 99% pure n-eicosane paraffin, which are cast in place by using the conductivity cell as a mold. The conductivity is determined as a function of the mean temperature of the specimen, and its sensitivity to a number of parameters is investigated. These include the presence or absence of vacuum during casting, the rate of solidification during casting, the thermal contact between the conductivity cell walls and the test specimen, the temperature difference across the specimen, the experimental site, and the aging of the apparatus and the paraffin. In supplementary experiments, the density of the solid paraffin and its melting temperature are determined. For specimens cast without vacuum, the thermal conductivity is virtually independent of the specimen temperature and of the solidification rate. However, for specimens cast under vacuum, the conductivity is found to be sensitive to the solidification rate, as is the density, and this dependence is attributed to the presence of entrapped gas bubbles. Comparison with the literature shows prior conductivity values for solid n-eicosane to be low, thereby explaining reported deviations between experimental and numerical results for solidification phase change.

INTRODUCTION

THE RESEARCH described in this paper was motivated by the design of heat storage devices which incorporate a phase change material (PCM). A primary design consideration is the rate at which energy can be extracted from or absorbed by the storage device. The energy flow rate is dependent on the system geometry, the initial and boundary conditions, and the thermophysical properties of the PCM and the storage device. Considerable work has been performed in the past to examine the effect of different geometries and boundary conditions on the energy flow from/to a PCM, as summarized in the survey articles [1, 2] and exemplified by specific research studies [3–5].

Attempts to correlate experimental and numerical results indicate that the accuracy of the values used for the thermophysical properties of the PCM can have a very important effect on the degree of correlation. A case in point is the experimental and numerical studies of phase change at the University of Minnesota involving the paraffin n-eicosane as the PCM. These studies will now be reviewed to set the stage for the present work.

In ref. [3], heat transfer experiments were performed which investigated the solidification of an initially superheated or non-superheated liquid in a cooled, thin-walled vertical tube. The solidification process was initiated by a step change in temperature at the outer surface of the tube. For the no-superheating case, the solidification is one-dimensional and radially inward, and for that case, numerical solutions were also performed. A comparison of the experimental and numerical results for the timewise variation of the position of the solidification front did not yield very good agreement (the data were about 25% above the numerical predictions). This outcome was attributed primarily to uncertainties in the values of the property group $k/\rho\lambda$ for the solid-phase n-eicosane, which was used in implementing the comparison. The thermal conductivity k was particularly suspect because of a 30% uncertainty in the published values [6]. Indeed, when the published k values were increased by 30%, better agreement between the solidification front data and predictions was achieved, but the data continued to fall above the predictions.

The experimental apparatus for the solidification studies performed in ref. [4] was altogether different from that of ref. [3], and a different batch of the n-eicosane PCM was used. However, as a special case, one-dimensional, radially inward solidification was achieved, and the solidification front data were in virtually exact agreement with those measured in ref. [3]. Furthermore, a one-dimensional numerical simulation based on immobilization of the freezing front, a scheme which differed fundamentally from that of ref. [3], totally validated the numerical predictions of

NOMENCLATURE

k	thermal conductivity
Q	rate of heat transfer
r_1	inner radius of conductivity specimen
r_2	outer radius of conductivity specimen
T_m	mean temperature of conductivity specimen, $(T_1+T_2)/2$
T_1	inner temperature of conductivity specimen
T_2	outer temperature of conductivity specimen.

Greek symbols

λ	latent heat of fusion
ρ	density of solid.

ref. [3]. In still another apparatus and with another batch of the PCM [7], data for one-dimensional, radially inward solidification agreed very well with that of ref. [4].

A sophisticated, all-numerical study of transient two-dimensional solidification of a PCM in a vertical, cylindrical capsule was performed in ref. [5]. One-dimensional, radially inward solidification was run as a special case, and the resulting numerical predictions were in excellent agreement with those of refs. [3, 4]. Not unexpectedly, the data of refs. [3, 4, 7] continued to disagree with the numerical predictions of ref. [5]. The authors of ref. [5] attributed the lack of agreement to the inaccuracy of the available information for the thermophysical property group $k/\rho\lambda$ for the solid phase of n-eicosane. To redress the inaccuracy, they forced agreement between the numerical predictions and the experimental data for the timewise variation of the position of the solidification front. The forced fit was achieved by multiplying the literature value of $k/\rho\lambda$ by a factor of 1.52, where the k value was that obtained by extrapolation of the k vs T values of ref. [6] to the melting temperature. Furthermore, it was felt that the main contribution to the correction factor was the uncertainty of the solid-phase conductivity value.

The two-dimensional capability of the model employed in ref. [5] was also used to generate numerical predictions for the solidification front when natural convection was present in the superheated liquid phase. These predictions were compared with the corresponding experimental data from ref. [3], and excellent agreement prevailed provided that the aforementioned property shift was made. This agreement furnishes independent confirmation of the hypothesis that the solid-phase property values of n-eicosane are in need of more accurate determination.

The total body of evidence from the aforementioned studies indicates that the uncertainty in the literature values of the thermophysical properties of solid n-eicosane [6, 8] was the main reason that the numerical and experimental results for solidification did not agree. This evidence and the published uncertainty ($\sim 30\%$) in the conductivity [6] strongly suggests that the thermal conductivity is the thermophysical property most in need of investigation. The present research was undertaken to determine definitive results for the thermal conductivity of the solid phase of n-eicosane as a function of temperature.

To fulfill this objective, a thermal conductivity cell was designed and fabricated which was virtually free of extraneous heat losses. It was used to measure the conductivity of solid n-eicosane as a function of temperature in the expected operating range of thermal storage devices, that is, from 10°C to the melting temperature of n-eicosane (approximately 35°C). To establish the generality of the results, measurements were made to examine the sensitivity of the conductivity to possible differences in the micro- and macrostructure of the material. Such structural differences may result from different solidification conditions including the rate of solidification and the presence or absence of a vacuum. Correspondingly, experiments were conducted in which the solidification rate was varied parametrically for solidification either under a partial vacuum or at ambient pressure (i.e. no vacuum). The n-eicosane used in the experiments was designated as 99% pure by the manufacturer.

The conductivity experiments were complemented by additional experiments which included an exploration of the possible role of thermal contact resistance between the solid paraffin and the bounding surfaces of the conductivity cell, the measurement of the melting temperature of n-eicosane, the determination of the solid-phase density for vacuum and no-vacuum solidification, and the assessment of aging effects and the site of the experiments.

EXPERIMENTAL APPARATUS

In the design and fabrication of the thermal conductivity cell, steps were taken to eliminate the causes of error which commonly occur in conductivity determinations. These include unaccounted for (or improperly estimated) heat losses, transient effects due to variations in the experimental environment, and uncertainties in the physical dimensions of the apparatus. The heat loss problem was made insignificant by using a spherical annulus as the conductivity cell as shown in Fig. 1. In this cell, the inner surface of the annulus was heated to a controlled uniform temperature, while the outer surface was cooled to a lower uniform temperature. Aside from

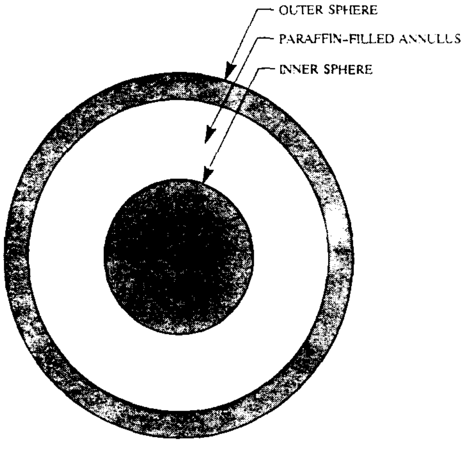

FIG. 1. Spherical conductivity cell.

extremely fine wires (thermocouple and power leads) the heat-carrying effects of which were shown by calculation to be negligible, heat which leaves the inner boundary of the annulus reaches the outer boundary via conduction through the n-eicosane paraffin.

Possible transient variations due to environmental conditions were minimized in two specific ways. First, the chosen environment was a large-volume water bath which, with appropriate controls, could be kept at a constant temperature independent of the variations in the laboratory temperature. Second, temperature and power data were collected over a period of several hours by a computer-controlled data acquisition system. This system enabled both the raw and reduced data to be plotted while a particular data run was in progress. An examination of the plots indicated when the transients in the conductivity apparatus due to imposed changes at the beginning of a data run had died away.

The physical dimensions of the apparatus were controlled to high accuracy by the use of a numerically controlled lathe to precisely machine the inner and outer spheres which bounded the paraffin-filled annulus. The concentricity of the inner and outer bounding surfaces was assured by use of a precision-machined positioning plate. Furthermore, the relatively large thickness of the annular gap (1.500 in., 3.810 cm) minimized the possible significance of dimensional uncertainties.

As will be elaborated later, the inner and outer spheres not only served to bound the solid paraffin specimen during the conductivity determination, but they also served as the walls of a mold into which liquid paraffin had been introduced and then solidified to form the specimen.

With measured temperatures T_1 and T_2 at the inner and outer bounding surfaces and heat transfer rate Q from the electric heating at the inner surface, the thermal conductivity k was evaluated from

$$k = Q(r_2 - r_1)/4\pi(T_1 - T_2)r_1 r_2. \qquad (1)$$

Here, k represents the mean conductivity for the temperature range between T_1 and T_2. For the present experiments, $r_1 = 1.500$ in. (3.810 cm) and $r_2 = 3.000$ in. (7.620 cm). All the quantities appearing on the right-hand side of equation (1) were known to high accuracy.

The following is a general description of the key features of the experimental apparatus. A complete description is available in the thesis [9] on which this paper is based.

Inner and outer spheres

The inner sphere was made up of two hemispheres which were precisely mated at their horizontal equators. Both hemispheres were fabricated to precise dimensions from a solid cylinder of aircraft-grade aluminum using a numerically controlled lathe. The assembled sphere had an outer radius of 1.500 in. (3.810 cm) and a 0.500 in. (1.270 cm) thick wall. The relatively thick wall of the sphere was chosen to enhance outer-surface temperature uniformity. After the machining, the outer surface of the sphere was polished using a succession of polishing compounds—finishing with a grit of 1200.

The inner surface of the sphere was heated by passing a current through a high-resistance wire embedded in a spiral groove that had been milled into the surface. Four chromel–constantan thermocouples, made from pre-calibrated 0.003 in. (0.0076 cm) diameter wire, were installed in latitudinal grooves milled in the outer surface of the sphere. The thermocouple junctions were positioned so that they lay on a great circle which passed through the poles. The wires were laid in the grooves and held in place by copper-oxide cement. Once the cement had cured, the surface of the cement was sanded flush with the surface of the sphere.

The outer sphere was also an assembly of two hemispheres intimately mated at their horizontal equators, also machined on a numerically controlled lathe from aircraft-grade aluminum. The sphere had an inner radius of 3.000 in. (7.620 cm) and a wall thickness of 0.500 in. (1.270 cm). The wall thickness was chosen both to enhance inner-surface temperature uniformity and to provide sufficient thermal mass to damp out possible small variations in the temperature of the water bath in which the outer sphere was immersed during the experiments. The inner surface of the sphere was polished after the machining, while the outer surface was painted with a waterproof epoxy to prevent corrosion from exposure to the water bath.

Seven thermocouples were installed flush with the inner surface of the outer sphere. These thermocouples were made from the same calibrated rolls of wire used for the inner-sphere thermocouples.

To support the outer sphere in the water bath, a stand was fabricated which provided positive positioning while enabling free circulation of the water between the stand and the sphere.

Setups for casting the paraffin test specimen

As noted earlier, the solid paraffin test specimen was formed by a casting process in which the con-

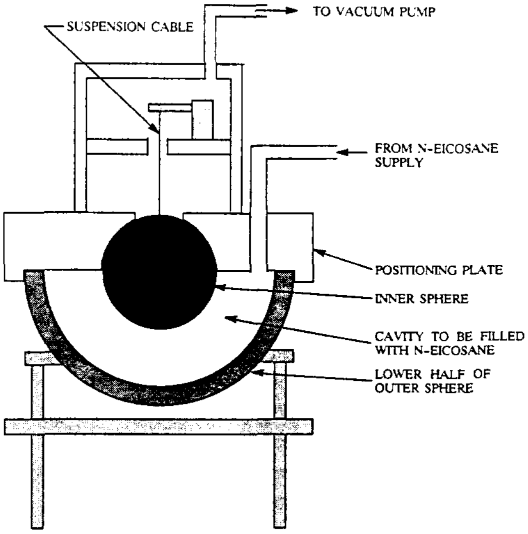

FIG. 2. Apparatus setup for first stage of casting.

ductivity-cell walls served as the mold. To guarantee precise positioning and concentricity of the inner and outer spheres, a two-stage casting procedure was devised. In the first stage, the casting of the lower half of the paraffin annulus was accomplished. During this stage, the upper half of the outer sphere was removed, and a specially fabricated positioning plate was put in place to mechanically fix the position of the inner sphere with respect to the lower half of the outer sphere. When the lower half of the paraffin annulus had solidified, it locked in the position of the inner sphere. The positioning plate was then removed, and the upper half of the outer sphere was put in place, after which the casting of the upper half of the paraffin annulus was accomplished.

The setup of the apparatus for the first stage of the casting procedure is shown diagrammatically in Fig. 2. The key components in this setup are the inner sphere, the lower half of the outer sphere, and the positioning plate which serves to fix the positions of the inner and outer spheres.

The positioning plate was a contoured disk, 1.75 in. (4.45 cm) thick and 3.75 in. (9.53 cm) in outer radius, which had been fabricated from plexiglass using a numerically controlled lathe. Plexiglass was chosen because of its transparency to light in the visible spectrum. This transparency served two purposes. First, it enabled a conventional heat lamp to be used to keep the free surface of the poured n-eicosane in the liquid phase while the rest of the n-eicosane solidified, thereby avoiding formation of sub-surface voids. Second, it allowed visual inspection of the progress of the solidification process and, in particular, the determination of when solidification was complete. The thickness of the plate was chosen to ensure dimensional stability and to provide sufficient depth to accommodate a series of contoured surfaces which were machined into its lower face.

The innermost of these contoured surfaces was a spherical cradle designed to house and position the inner sphere. The diameter of the cradle was equal to that of the sphere. Further out, near the rim, flats and shoulders were machined in the plate to force concentricity of the spheres in the setup shown in Fig. 2. The inner sphere was held firmly in the cradle by a subassembly mounted atop the positioning plate as illustrated in the figure. The main components of the subassembly were a guitar-string tightener and a suspension cable attached to the top of the inner sphere. Turning the tightener forced the inner sphere into the cradle.

The positioning plate was also fitted with two access tubes. One was for filling the space between the inner sphere and the lower half of the outer sphere with liquid n-eicosane from the supply reservoir. The other provided a means to connect the suction line of a vacuum system to the positioning plate.

As noted earlier, the positioning plate was removed when the n-eicosane had fully solidified in the lower half of the inter-sphere space, and the upper half of the outer sphere was put in place. The setup for casting the upper half of the paraffin annulus is shown in Fig. 3. As seen there, a reservoir containing liquid n-eicosane was threaded through a temporary aperture at the top of the outer sphere. Liquid n-eicosane was introduced into the reservoir by a plexiglass tube attached to its side. The reservoir maintained a continuous supply throughout the solidification process to ensure the absence of voids which otherwise would have formed due to the shrinkage of the paraffin.

The reservoir was fitted with a cap which included a proportionally controlled electric immersion heater and a vacuum fitting. The immersion heater extended downward through the reservoir and into the mold cavity to within 0.5 in. (1.27 cm) of the inner sphere. By setting the proportional controller to a temperature just above the solidification temperature, a liquid surface was maintained in the mold cavity and a path was provided for liquid flow from the reservoir to the cavity.

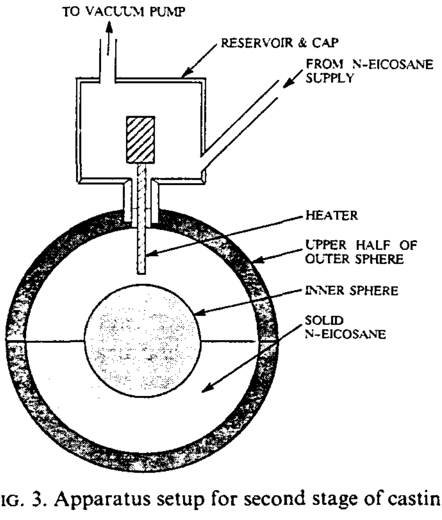

FIG. 3. Apparatus setup for second stage of casting.

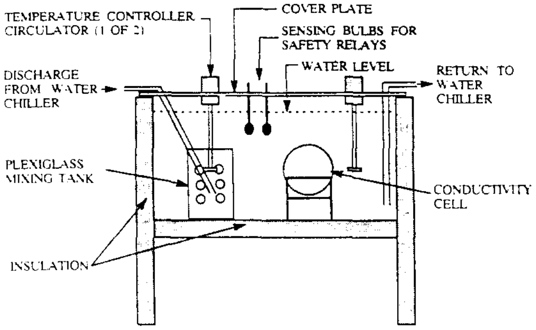

FIG. 4. Conductivity cell in the water bath during a conductivity measurement.

Water-bath test environment

To maintain the outer sphere of the conductivity cell as an isothermal heat sink, the entire cell was immersed in an agitated, constant-temperature water bath as shown in Fig. 4. The bath was contained in a rectangular stainless steel tank the length, width, and depth of which were 21 × 16 × 15 in. (53 × 40 × 38 cm). The tank was insulated on the sides and bottom with 4 in. (10 cm) of fiberglass, and during a data run, the top of the tank was capped with a plastic-covered sheet of insulation.

As seen in the figure, two temperature controller/water circulator units were suspended in the water bath. One of these units was positioned so that its heater and water discharge port were situated inside a vertical plexiglass cylinder which rested on the bottom of the tank. A supply of chilled water from a water chiller was also ducted into the cylinder. The cylinder functioned as a mixing chamber for the heated and chilled water. Holes were provided in the cylinder wall to enable the mixed fluid to escape into the water bath proper. The temperature control function of the second controller/circulator was deactivated so that it acted only as a circulator to provide highly agitated water at the surface of the outer sphere.

The conductivity cell, temperature controller/circulator units, and water chiller were protected from temperature excesses by a system which sensed and compared the water-bath temperature with set-point values.

Vacuum system

In preliminary solidification experiments performed here at atmospheric pressure as well as in similar experiments in ref. [10], visual inspection of the resulting solid n-eicosane revealed the presence of small bubble-like voids distributed throughout the solid. It was hypothesized that these voids resulted when air that had been dissolved in the liquid was trapped in the solid during solidification. To draw off the air, a vacuum system was designed so that storage, transport, and solidification of the liquid were performed under a continuous vacuum. The extent of the vacuum was limited by the vapor pressure of the liquid n-eicosane at the storage temperature (vacuum of approximately 20 in. Hg at 50°C).

The apparatus used to generate and control the vacuum included a vacuum pump, gauge, valves, and the piping necessary to interconnect the supply reservoir, the vacuum pump, and the solidification setup.

Power supply and data acquisition systems

The function of the power supply system was to provide a very well controlled, highly stable voltage to the electrical resistance heater inside the inner sphere. To this end, two regulated power supplies were used in series, with the building a.c. voltage being first passed to an a.c. supply which, in turn, fed a d.c. supply. With this arrangement, it was possible to convert a conventional fluctuating a.c. building voltage supply to a d.c. output that was steady to 0.0001 V for a nominal 10 V output (0.001% stability).

The d.c. supply was wired in series with a calibrated resistor (current shunt) and the heater in the inner sphere. The power supplied to the heater was determined from the voltage drops across the resistor and across the voltage taps soldered to the heater lead wires. Both of these voltages were read by the data acquisition system.

The data acquisition system not only read the aforementioned heater power voltages but also the thermocouple voltages associated with the temperatures of the inner and outer spheres. The data were acquired by an analog-to-digital converter (HP 3421A) controlled by a program executed by a personal computer (HP 86B).

The control program stored the voltages on a disk, converted the thermocouple voltages to temperatures, performed the data reduction, stored the reduced data on a disk, and plotted thermal conductivity vs time on the computer monitor. The program executed the foregoing steps every 5 min during a conductivity run, yielding information which enabled the experimenter to determine when a specific conductivity determination was complete or when an adjustment of the water bath or of the heater power was necessary.

EXPERIMENTAL PROCEDURE

The experimental procedures used for the conductivity measurements are distinguished by the different casting and solidification scenarios used to form the spherical annulus of solid n-eicosane paraffin. For all cases, the two-stage casting procedure discussed earlier in the paper was used, supplemented by specific protocols to define each scenario. Special care was taken to ensure that the end result of each casting/solidification scenario was a test specimen which fully filled the inter-sphere space at the casting temperature (i.e. the temperature imposed at the outer surface of the cell during casting). The scenarios will be outlined in the following paragraphs, with full details available in ref. [9].

Four different scenarios were employed. In the first, the casting was accomplished with the conductivity cell in the water bath and with all procedures carried out at atmospheric pressure (no vacuum). Care was taken to vent any air that may have been entrapped during the filling of the mold. The second scenario differed from the first by the imposition of a 20 in. Hg vacuum on the n-eicosane while it was in the supply reservoir, while it was transported to the mold cavity, and during its solidification in the cavity. For both of these scenarios, the rate of solidification was controlled and varied by setting the temperature of the water bath (thereby defining the casting temperature).

The third scenario was employed to further explore the effect of solidification rate for a given casting temperature. To obtain an extremely slow rate of solidification, the convective heat transfer coefficient at the outer surface of the cell was changed from that for forced convection in water (i.e. the agitated water bath) to natural convection in air. The air-environment casting was performed without vacuum at two different ambient temperatures, namely, 10 and 20°C, respectively in a refrigerator and on a laboratory bench.

As already noted, the different solidification rates and the vacuum vs no-vacuum solidification were intended to provide information on the sensitivity of the thermal conductivity to the micro- and macrostructure of the material. Furthermore, as will be elaborated later, the use of different casting temperatures enables inferences to be drawn about the thermal contact between the paraffin specimen and the bounding spherical surfaces. The concern about thermal contact motivated the fourth scenario. This scenario included an additional operation prior to the regular no-vacuum casting procedure. It involved precoating the inner surface of the upper half of the outer sphere with a thin layer of n-eicosane that was allowed to cool slowly. The concern was that in the usual procedure, the surface in question was below the solidification temperature when the liquid was introduced into the mold cavity, and the possible rapid freezing adjacent to the surface might have caused imperfect surface contact.

A decision to determine the density of the solid phase of n-eicosane as a function of solidification temperature and of the presence or absence of vacuum was made following examination of the thermal conductivity results. The density determinations were performed for temperatures which ranged from 15 to 33°C. To accomplish this, equipment was assembled to solidify the paraffin in such a manner that Archimedes' principle could be used to determine the density [9]. Samples of paraffin under vacuum and not under vacuum were solidified at the same time in glass test tubes immersed in a temperature controlled, agitated water bath. The mass of the solid was determined while it was suspended in air and while it was submerged in water using a balance with a resolution of 0.001 g.

The melting temperature of n-eicosane was determined from visual observations of specimens contained in specially fabricated cylindrical capsules made of plexiglass. To investigate the onset of melting, the capsules were positioned in a temperature-controlled, agitated water bath. The bath temperature was systematically increased in 0.1°C intervals and held at each temperature level for 24 h.

The thermal conductivity experiments were performed at two separate sites. The research was begun at the University of Minnesota (UM) and later continued and concluded at Bucknell University (BU), with the same conductivity cell used for all of the experiments. The major differences between the sites included the degree of thermal stability of the respective laboratories, the data acquisition systems, and the sources of chilled water. Replicate data runs were made at the two sites to verify the site independence of the results.

RESULTS AND DISCUSSION

The thermal conductivity k of solid n-eicosane was determined as a function of the arithmetic mean T_m of the inner and outer surface temperatures of the annular specimen. For each of the casting/solidification scenarios described in the preceding section of the paper, T_m was varied from the casting temperature to a value near the melting temperature. In what follows, the conductivity results will be presented graphically with k along the ordinate and T_m along the abscissa. The data will be parameterized by the casting temperature and by the casting/solidification scenario. In particular, for a specified scenario, the data corresponding to a specimen formed at a given casting temperature will be represented by a common data symbol. In the characterization of the data, the designations UM and BU respectively refer to conductivity experiments performed at the University of Minnesota and at Bucknell University. For all cases, the temperature difference $(T_1 - T_2)$ across the specimen was in the range of 2°C.

Casting/solidification without vacuum

The thermal conductivity results for specimens formed by casting/solidification at atmospheric pressure (i.e. without vacuum) are presented in Fig. 5. Initial attention will be given to Fig. 5(a), which conveys results corresponding to casting/solidification with the mold (i.e. the conductivity cell) immersed in the agitated water bath.

The three data sets appearing in Fig. 5(a) correspond to casting temperatures of approximately 10, 20, and 30°C. The conductivity values for the specimen cast at 10°C are virtually constant as T_m increases from approximately 10 to 32.5°C. The average value for these points is 0.4224 W m^{-1} °C^{-1}, with individual deviations from the average being less than 1%. At temperatures above 32.5°C, the single data point at 33.8°C indicates a decrease of k as the temperature

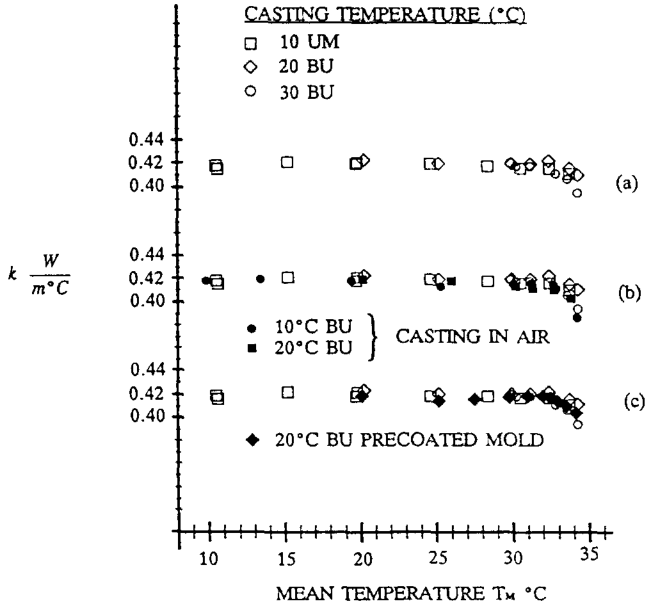

FIG. 5. Conductivity results for solid n-eicosane cast at atmospheric pressure (i.e. without vacuum): (a) conductivities for specimens cast in the water bath; (b) conductivities for specimens cast in air compared with (a); (c) conductivities for specimen cast in a precoated mold compared with (a).

increases; the decrease is approximately 1.7% of the aforementioned average value. For the specimen cast at 20°C, the conductivity values again remain constant from the casting temperature to a temperature near 32.5°C. The average of these conductivity values is 0.4248 W m^{-1} °C^{-1}, which is about 0.5% above the average for the k values associated with the 10°C casting. The two measured conductivity values above $T_m = 32.5$°C decrease with increasing temperature. At 34.3°C, k has decreased by 2.5% relative to the aforementioned average for this casting temperature. In the temperature range 30–32.5°C, the conductivity values for the specimen cast at 30°C are very similar to those previously discussed (average value of 0.4231 W m^{-1} °C^{-1}) and, as before, the conductivity drops off at $T_m > 32.5$°C.

An overall average of all the k values in Fig. 5(a) below 32.5°C yielded 0.4234 W m^{-1} °C^{-1}, with an extreme deviation from the average of about 0.9%. Therefore, in this range, the conductivity is independent of the temperature T_m of the specimen and also of the casting temperature at which the specimen was formed.

This finding suggests two inferences. The first is related to the fact that different casting temperatures give rise to different solidification rates during the casting process. Yet, despite the different solidification rates and possible differences in the resulting microstructure of the material, k was unaffected. Thus, tentatively, k does not appear to be sensitive to the solidification rate (this issue will be elaborated shortly).

The second inference relates to contact resistance. At a given T_m, it may be conjectured that specimens formed at different casting temperatures might experience different degrees of contact with the bounding spherical surfaces. This is because of the different coefficients of thermal expansion for the paraffin and for the aluminum bounding walls (respective nominal values of 0.0003°C^{-1} [11] and 0.000024°C^{-1} [12]). However, the fact that k was the same regardless of the casting temperature suggests that the thermal contact was so good as not to be affected by the different expansion rates.

For $T_m > 32.5$°C, where the conductivity values in Fig. 5(a) decrease with increasing temperature, there is also a tendency of the data to spread (2.3% at 33.5°C). Two possible reasons may be offered for the decrease: (1) the existence of a 'solid–solid phase modification transition (the triclinic crystal structure of the paraffin is converted to a hexagonal structure)' as described in ref. [13] and (2) impurities in the n-eicosane. With regard to the latter, the presence of another substance that changes phase at a lower temperature than the n-eicosane could cause a change in the measured conductivity. The experimental determination of the melting temperature indicated that melting occurred over a finite temperature range rather than at a specific temperature, and visual observations suggested softening at 35.3°C which, in turn, suggested the possible presence of a liquid phase.

Attention will now be turned to Fig. 5(b), where the effects of solidification rate are further explored. For reference purposes, the data of Fig. 5(a) are reproduced in Fig. 5(b), i.e. the open symbols, while the new data are represented by black symbols. The new data correspond to specimens cast in air environments with respective ambient temperatures of approximately 10 and 20°C. The air-environment solidification times (16 and 20 h, respectively) were about

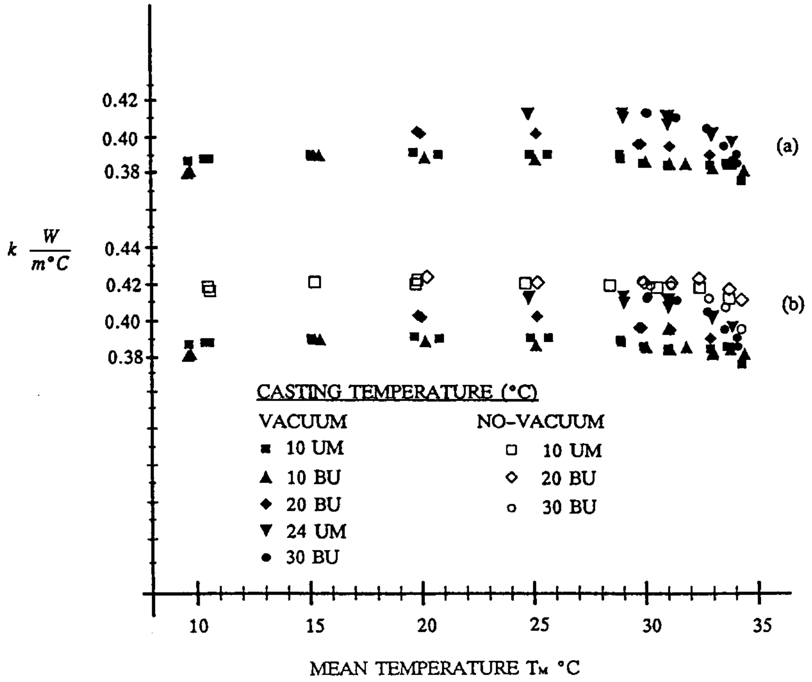

FIG. 6. (a) Conductivity results for solid n-eicosane cast under vacuum with the mold in the water bath: (b) comparison of conductivities for specimens cast with and without vacuum.

twice the solidification times in the water-bath casting procedure.

The data corresponding to the slower solidification rates follow the same pattern as the reference data. The average of the conductivity values for the slower solidification case differs from the average for the reference data by less than 0.5% in the T_m range extending from 9.8 to 32.7°C, and insensitivity to the casting temperature is also observed. Therefore, the insensitivity of the conductivity to the solidification rate, set forth tentatively in connection with Fig. 5(a), can now be regarded as a firmer conclusion. For $T_m > 32.5$°C, Fig. 5(b) confirms the slight decrease in k that was noted in Fig. 5(a).

Figure 5(c) conveys results of a further exploration of thermal contact. In the figure, the black data symbols correspond to the casting scenario which involved the precoating of the inner surface of the upper half of the outer sphere with a layer of n-eicosane (i.e. the fourth casting scenario). Also shown in the figure for reference purposes are the data from Fig. 5(a)—the open symbols. It is seen that very good agreement prevails between the black and open data symbols. This finding supports the earlier inference, drawn from Fig. 5(a), that there was very good contact between the paraffin annulus and its bounding walls.

Casting/solidification under vacuum

Conductivity results are presented in Fig. 6 for specimens formed by casting/solidification under vacuum and with the mold immersed in the water bath. The conductivity determinations were made for specimens formed at casting temperatures of approximately 10, 20, 24, and 30°C. The data are plotted as black symbols in both Figs. 6(a) and (b). For reference purposes, Fig. 6(b) also includes as open symbols the data from Fig. 5(a); those data correspond to casting without vacuum and with the mold in the water bath. Thus, the distinguishing feature between the black and open symbols in Fig. 6(b) is the presence or absence of vacuum during the casting process.

An overview of Fig. 6(a) indicates a dependence of the conductivity on the casting temperature of the specimen. In particular, at a fixed T_m, there is a tendency for the conductivity to increase with the casting temperature. The extent of the increase relative to the k value for the 10°C casting (at a given T_m) is about 2% for the 20°C casting and about 5% for the 25°C casting. These percentages decrease as T_m increases. The conductivity values corresponding to casting at 25 and 30°C are very similar, with differences of less than 1% for the entire range of T_m over which data were collected.

The conductivity values which correspond to a given casting temperature remain fairly constant (within ±1%) from the casting temperature to approximately 32°C. Indeed, for the 10°C casting case, the near constancy persists to 34°C, after which there is about a 2% decrease. For the other cases, the conductivity declines with increasing T_m beyond 32°C. The decline is largest for the data corresponding to

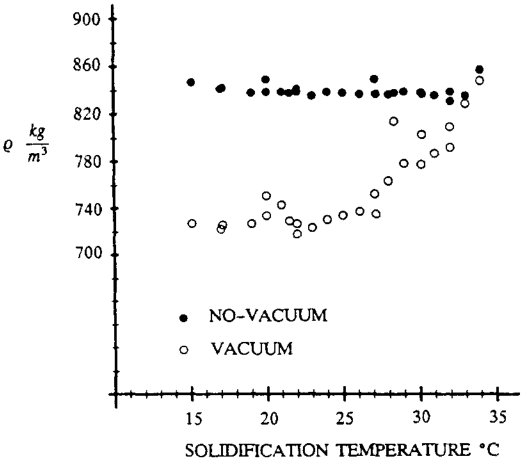

FIG. 7. Density of solid n-eicosane solidified either at atmospheric pressure (i.e. without vacuum) or under vacuum.

the 30°C casting—about 5%. The decline in conductivity as T_m approaches the melting temperature can be attributed to the same factors as were discussed in connection with the no-vacuum results.

Attention is next turned to the comparison of results corresponding to with-vacuum and no-vacuum casting conveyed in Fig. 6(b). At any T_m in the investigated range, k for no-vacuum casting is consistently above k for with-vacuum casting. Also, as already noted, the sensitivity of the with-vacuum k to casting temperature is much greater than that for the no-vacuum k. The difference between the conductivity values corresponding to the two casting methods can be quantified by comparing the respective average values for the range of T_m from 10 to 32°C. For casting at 10, 20, and 25/30°C, the with-vacuum k values are 7, 5, and 2% less than the no-vacuum k value.

A possible explanation for the different conductivity values corresponding to the with-vacuum and no-vacuum casting as well as for the sensitivity of the with-vacuum results to the casting temperature is a variation in the composition of the solid. One possible cause of a variation in composition would be the presence of trapped gases in the solid. If the conductivity of the gases were lower than that of the solid, then the measured conductivity of the mixture would also be lower. Since the presence of trapped gases would also affect the density of the mixture, a measured variation of density can be used to indicate a variation in composition. It was this reasoning which motivated the density determinations, the results of which will now be reported.

Density results and their conductivity-related implications

The measured density of solid n-eicosane is plotted in Fig. 7 as a function of the solidification temperature (i.e. of the rate of solidification). At each solidification temperature, there are two data points, one representing the density of a sample solidified under vacuum and the other representing the density of a sample solidified at atmospheric pressure (without vacuum).

From the figure, it is seen that the density of n-eicosane solidified without vacuum is virtually independent of the solidification temperature (as was the thermal conductivity). The greatest variation is about 1.1% about a mean value of 840 kg m^{-3}. On the other hand, the density of the n-eicosane solidified under vacuum varies irregularly with increasing temperature from 729 kg m^{-3} at 15°C to 738 kg m^{-3} at 26°C. From 26 to 34°C, there is a clearly increasing tendency, with the density at 33°C (830 kg m^{-3}) being nearly the value of the corresponding no-vacuum sample. In the temperature range of 20–22°C, there is a small rise and fall of the density (3.5% of the immediately preceding and following values). A possible explanation of this anomaly was found in the article by Kolesnikov and Syunyaev [13]. They reported a solid–solid phase change on cooling (solidification) in this temperature range. This was the same solid–solid phase change (hexagonal to triclinic) discussed earlier in connection with the decrease in thermal conductivity near the melting temperature, except that it occurs at a lower temperature in solidification due to a supercooling effect [13].

The no-vacuum density results measured here are in the same range as those reported in the literature, which includes 856 kg m^{-3} at 34°C [11], 910 kg m^{-3} at 10°C to 856 kg m^{-3} at 34°C [14], and 848.95 kg m^{-3} at 36.39°C [15].

The data of Fig. 7 can be put into physical perspective by noting that during solidification, it was observed that there were many bubbles adhering to the liquid–solid interface under vacuum conditions, while without vacuum, there were few, if any, bubbles. The number of bubbles visible at the interface in the presence of vacuum increased as the solidification temperature decreased and with increased vacuum.

The density experiments established that the n-eicosane solidified under vacuum had a lower density (more voids in the solid) than that solidified without vacuum. The density data were used to calculate the volume fractions of the gas in the samples solidified under vacuum. The volume fractions were then employed in a simple model of a composite material to calculate an estimate of the conductivities of the composite. This model assumes that at any cross section, the area fraction occupied by the gas is the same as the volume fraction of the gas. With this assumption, the conductivity of the composite is found by summing the product of the conductivity and the volume fraction for each of the components. The average k value for the no-vacuum results (0.4234 W m^{-1} °C^{-1}) was used for the n-eicosane, and the k value for the gas was that of air at the solidification temperature. The results obtained from this calculation are plotted as the star data symbols in Fig. 8 at the solidification temperature corresponding to the density data. Also shown in Fig. 8 is the with-vacuum

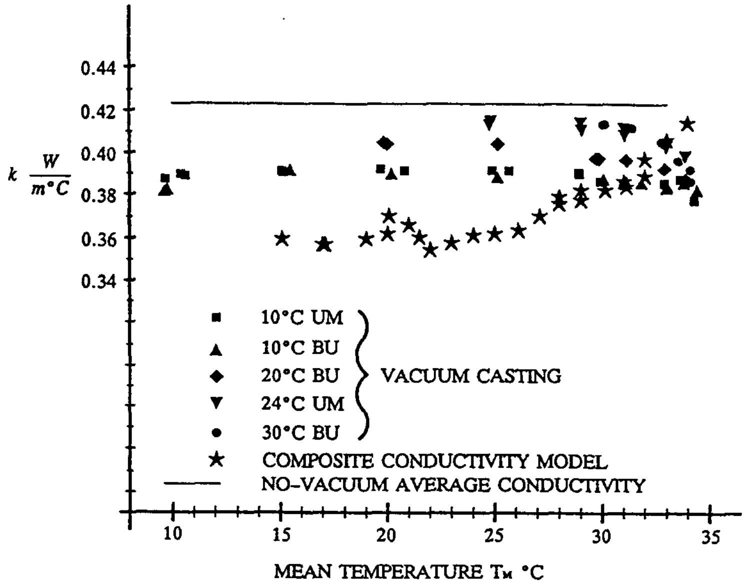

FIG. 8. Comparison of experimentally determined conductivity results for solid n-eicosane with predictions from a model for a solid–gas composite.

conductivity data and a line representing the average of the no-vacuum conductivity values.

Inspection of the figure shows that the conductivity results from the composite model display a temperature dependence which is similar to that for the with-vacuum density data of Fig. 7. For the most part, the composite-model conductivity is less than the with-vacuum conductivity values. The exception occurs at higher temperatures, where impurity effects may play a role. Of particular significance is the fact that both the composite-model and with-vacuum conductivities increase with increasing casting/solidification temperature and that both are below the conductivity value for the no-vacuum case.

Although the composite conductivity model is a simple one, it explains the lower conductivity values obtained for the n-eicosane specimens with the vacuum-casting scenario. However, a strict quantitative comparison is not possible because the casting/solidification procedures used for the thermal conductivity experiments and for the density experiments were different.

Accuracy verifications

Figure 9 is presented to further verify the accuracy of the thermal conductivity results. One issue is whether the data were sensitive to the value of the temperature difference $(T_1 - T_2)$ between the inner and outer surfaces of the n-eicosane. The temperature difference could affect the results in two ways: (1) by shifting the temperature with which the conductivity value is associated and (2) by altering the precision of the data. This issue is explored in Fig. 9(a), where results for two temperature differences are presented, nominally 1.8 and 2.5°C, respectively represented by the black and the open data symbols. For each data set characterized by a given casting temperature, at each T_m, there is no difference (to three significant figures) in the conductivity values for the two temperature differences. For all the conductivity determinations performed throughout the present investigation, the data were collected at temperature differences between these two values.

The effect of site and aging on the conductivity results is explored in Fig. 9(b), which shows two sets of conductivity values, one determined from data collected at the University of Minnesota and the other from data collected at Bucknell University. The relevant differences between these sites were noted earlier in the paper. The data correspond to with-vacuum casting at 10°C. As the figure indicates, there is virtually no difference between the two data sets over the entire range of T_m. This indicates no sensitivity of the data to the experimental site or to the differences in experimental equipment. Furthermore, since there was a time lapse of about a year between the two data sets, it can be concluded that there was no effect of aging of either the apparatus or the paraffin.

Comparison with literature values

The only reported values for the thermal conductivity of the solid phase of n-eicosane are those of ref. [6] for four temperatures ranging from 293 to 307 K. The four conductivity values of ref. [6] are plotted in Fig. 10 along with the present results from Fig. 5(a) (casting without vacuum, in the water bath). As seen in Fig. 10, the present k values are consistently well above the literature values from ref. [6]. Furthermore, the latter decrease steadily with increasing T_m, in contrast to the near constancy of the k values found here.

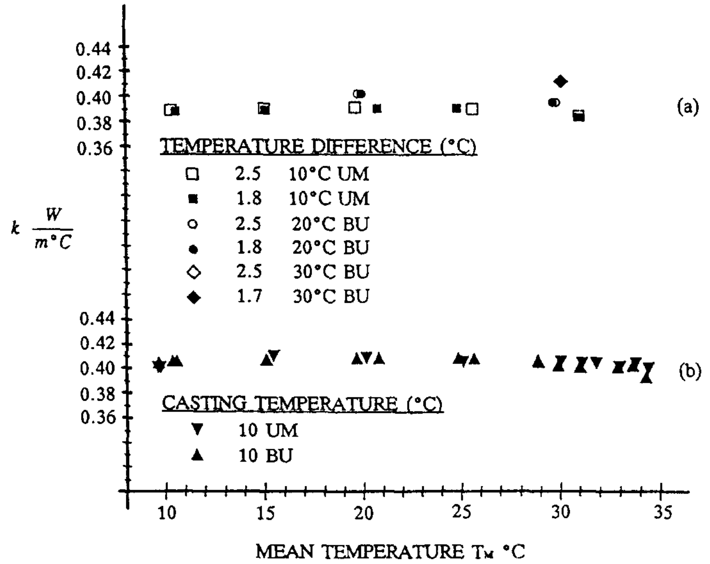

Fig. 9. (a) Conductivity results for solid n-eicosane for two values of the temperature difference across the specimen (specimens cast under vacuum); (b) examination of the effects of site and aging on the conductivity results (specimens cast under vacuum).

A concentric cylindrical conductivity cell was used in ref. [6] to measure the thermal conductivity of the solid phase of n-eicosane. Although a brief description of the apparatus is given in ref. [6], there is no description of the methodology used for preparation and solidification of the specimen (in particular, no mention was made of the use of vacuum). Furthermore, the authors of ref. [6] estimated that errors in their temperature measurements could be as high as 20%. When this temperature error was combined with other unspecified errors, the estimated error bound for their results was stated to be ±30%. Because of these uncertainties, it is not possible to provide a definitive explanation of the differences between the present results and those of ref. [6].

CONCLUDING REMARKS

It is now appropriate to revisit the issue which motivated the present research. As noted in the Introduction, in the literature, when available thermophysical property data for solid n-eicosane were used to implement a comparison of experimental and numerical results for solidification phase change, good agreement was not achieved. The comparison involved the property group $k/\rho\lambda$, where the value of

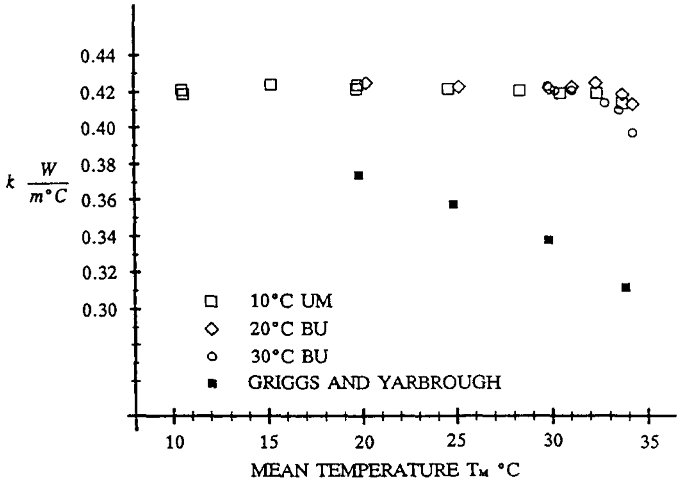

Fig. 10. Comparison of present conductivity results (specimens cast without vacuum, in the water bath) with those of Griggs and Yarbrough [6].

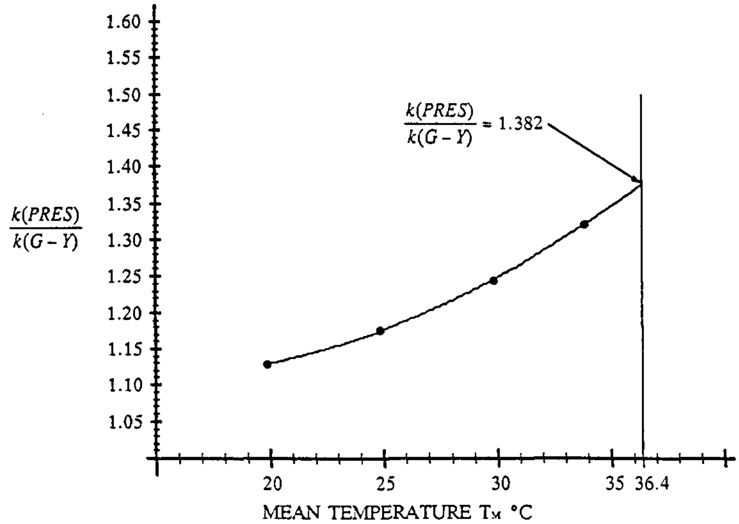

FIG. 11. Ratio of present conductivity results (specimens cast without vacuum, in the water bath) to those of Griggs and Yarbrough [6].

k had been obtained by extrapolating the data of ref. [6] to the melting temperature. To force agreement between the experimental and numerical results, the value of $k/\rho\lambda$ based on the then-available property data was multiplied in ref. [5] by a correction factor of 1.52.

The group $k/\rho\lambda$ will now be re-examined using the best property information available at present. The first step is to compare the present k value at the melting temperature with that of ref. [6]. The comparison is facilitated by Fig. 11. This figure presents the ratio formed by dividing the k values for the present no-vacuum case by those of ref. [6] at the four temperatures for which the latter are available. A least-squares quadratic equation, shown as the solid line in the figure, was fitted to the four points in order to extrapolate to the melting temperature. The equation was evaluated at $T = 36.4°\text{C} = 309.55$ K, which was the melting temperature employed in the data reduction in the solidification experiments of ref. [3]. The k ratio obtained from the extrapolation is 1.382, i.e. the present k value exceeds that of ref. [6] by 38.2%.

By using the k ratio of 1.382 and by making use of more accurate values of ρ and λ ($\rho = 840$ kg m^{-3}, measured here for the no-vacuum solidification, and $\lambda = 239.94$ kJ kg^{-1} from ref. [13]), a resulting value of $k/\rho\lambda$ is obtained which is 1.44 times that of ref. [3]. This value is close to the factor of 1.52 that was applied in ref. [5] to force fit experimental and numerical results. Thus, the present conductivity data support the magnitude of the force fit correction.

In addition to enabling definitive thermal conductivity information to be obtained for a specific substance (i.e. 99% pure n-eicosane paraffin), the present conductivity cell and its operational procedures hold high promise for application to other substances. In this regard, attention is called to the detailed design drawings of the apparatus and the painstaking account of the experimental procedure that are available in ref. [9].

REFERENCES

1. R. Viskanta, Phase-change heat transfer. In *Solar Heat Storage: Latent Heat Materials* (Edited by G. A. Lane), Chap. 5. CRC Press, Boca Raton, Florida (1983).
2. R. Viskanta, A. G. Bathelt and N. W. Hale, Jr., Latent heat-of-fusion energy storage: experiments on heat transfer during solid–liquid phase change. In *Alternative Energy Sources III. Solar Energy* (Edited by T. N. Veziroglu), Vol. 1, pp. 279–304. Hemisphere, Washington, DC (1983).
3. E. M. Sparrow and J. A. Broadbent, Freezing in a vertical tube, *J. Heat Transfer* **105**, 217–225 (1983).
4. E. D. Larson and E. M. Sparrow, Effect of inclination on freezing in a sealed cylindrical capsule, *J. Heat Transfer* **106**, 394–401 (1984).
5. E. M. Sparrow and Y. Ohkubo, Numerical predictions of freezing in a vertical tube, *Numer. Heat Transfer* **9**, 79–95 (1986).
6. E. I. Griggs and D. H. Yarbrough, Thermal conductivity of solid unbranched alkanes from n-hexadecane to n-eicosane, *Proc. 14th Southeastern Seminar on Thermal Sciences*, pp. 256–267 (1978).
7. J. S. Nelson, Effects of rotation on encapsulated freezing, Ph.D. Thesis, Department of Mechanical Engineering, University of Minnesota, Minneapolis, Minnesota (1984).
8. W. R. Humphries and E. I. Griggs, A design handbook for phase change thermal control and energy storage devices, NASA Technical Paper 1074 (1977).
9. P. C. Stryker, Precise measurement of the thermal conductivity of solid n-eicosane paraffin, Ph.D. Thesis, Department of Mechanical Engineering, University of Minnesota, Minneapolis, Minnesota (1989).
10. R. G. Kemink, Melting of a solid adjacent to a heated vertical cylinder with or without subcooling of the solid, Ph.D. Thesis, Department of Mechanical Engineering, University of Minnesota, Minneapolis, Minnesota (1981).
11. D. V. Hale, M. J. Hoover and M. J. O'Neill, Phase

change materials handbook, NASA Contractor Report, NASA CR-61363 (1971).

12. J. J. Tuma, *Handbook of Physical Calculations*. McGraw-Hill, New York (1976).
13. S. I. Kolesnikov and Z. I. Syunyaev, Phase transitions in the melting and crystallization of n-$C_{18}H_{38}$ and n-$C_{20}H_{42}$, *J. Appl. Chem. U.S.S.R.* **58**(10), 2097–2101 (1985).
14. Research and development study on thermal control by use of fusible materials, Northrop Corporation Interim Report NSL 65-16 to NASA-MSFC on Contract No. NAS 8-11163 (February 1965).
15. J. A. Broadbent, Melting and freezing in a vertical cylinder, M.S. Thesis, Department of Mechanical Engineering, University of Minnesota, Minneapolis, Minnesota (1982).

APPLICATION D'UNE CELLULE SPHERIQUE DE CONDUCTIVITE THERMIQUE AU n-EICOSANE SOLIDE

Résumé—Une cellule sphérique construite avec précision pour la mesure de la conductivité thermique est utilisée pour réaliser une conduction permanente monodimensionnelle à travers un échantillon en coquille. Les échantillons sont des solides en n-eicosane pur à 99% mis en place par moulage dans le cellule. La conductivité est déterminée en fonction de la température moyenne de l'échantillon et sa sensibilité à plusieurs paramètres est étudiée. On considère la présence ou l'absence du vide pendant le moulage, la vitesse de solidification pendant le moulage, le contact thermique entre les parois et l'échantillon, l'écart de température à travers l'échantillon, le site expérimental et le vieillissement de la paraffine. Dans des expériences supplémentaires, on détermine la masse volumique de la paraffine solide et sa température de fusion. Pour des spécimens moulés sans vide, la conductivité thermique est virtuellement indépendante de la température du spécimen et de la vitesse de solidification. Néanmoins pour des spécimens moulés sous vide, la conductivité est sensible à la vitesse de solidification comme l'est la masse volumique et cette dépendance est attribuée à la présence de bulles de gax piégées. Une comparaison avec la littérature montre des valeurs de conductivité faibles du n-eicosane solide, expliquant de ce fait des écarts entre des résultats numérique et expérimentaux pour le changement de phase à la solidification.

MESSUNGEN IN EINER KUGELIGEN WARMELEITFÄHIGKEITSZELLE AN FESTEM n-EICOSAN-PARAFFIN

Zusammenfassung—Es wurde eine präzis gearbeitete, kugelige Wärmeleitfähigkeitszelle verwendet, um eine gleichbleibende eindimensionale verlustfreie radiale Wärmeleitung in einem kugeligen Ringspalt zu erhalten. Die Wärmeleitfähigkeitszelle diente als Gußform für die untersuchten festen Materialien aus 99% reinem n-Eicosan-Paraffin. Die Wärmeleitfähigkeit wird als Funktion der mittleren Temperatur des Versuchsstoffes bestimmt. Außerdem wird der Einfluß einiger Parameter untersucht: Anwesenheit oder Abwesenheit von Vakuum während des Gießens, die Verfestigungsgeschwindigkeit während des Gießens, der thermische Kontakt zwischen der Wand der Wärmeleitfähigkeitszelle und dem Versuchsstoff, die Temperaturdifferenz im Versuchsstoff, der Versuchsort und schließlich die Alterung von Versuchsanlage und Paraffin. In ergänzenden Versuchen werden die Dichte des festen Paraffins und seine Schmelztemperatur bestimmt. Für Materialien, die ohne Vakuum gegossen worden sind, ist die Wärmeleitfähigkeit praktisch unabhängig von der Temperatur und der Erstarrungsgeschwindigkeit. Jedoch hängt bei Vakuum während des Gießvorgangs die Wärmeleitfähigkeit wie auch die Dichte spürbar von der Erstarrungsgeschwindigkeit ab, was auf eingeschlossene Gasblasen zurückgeführt wird. Literaturvergleiche ergeben, daß früher ermittelte Werte für die Wärmeleitfähigkeit von n-Eicosan niedriger sind als die hier bestimmten; damit können die festgestellten Abweichungen zwischen gemessenem und berechnetem Ergebnis für den Verfestigungsvorgang erklärt werden.

ПРИМЕНЕНИЕ СФЕРИЧЕСКОЙ ЯЧЕЙКИ ДЛЯ ИЗМЕРЕНИЯ ТЕПЛОПРОВОДНОСТИ В СЛУЧАЕ ТВЕРДОГО ПАРАФИНА Н-ЭЙКОЗАН

Аннотация—Прецизионная сферическая кондуктометрическая ячейка применяется для получения стационарной одномерной радиальной теплопроводности без потерь через кольцевой опытный образец. Исследуемые образцы твердого 99%-ного чистого парафина н-эйкозан отливаются с использованием кондуктометрической ячейки в качестве прессформы. Определяется коэффициент теплопроводности как функция средней температуры образца, и исследуется его зависимость от ряда параметров и условий, таких как наличие и отсутствие вакуума, скорость затвердевания при литье, тепловой конуакт между стенками ячейки и опытным образцом, разность температур в образце, место проведения эксперимента и старение аппарата и парафина. В дополнительных экспериментах определяются плотность твердого парафина и его температура плавления. В случае отливки образцов при отсутствии вакуума коэффициент теплопроводности практически не зависит от температуры образца и скорости затвердевания. Однако при отливке образцов в вакууме теплопроводность и плотность образца зависят от скорости затвердевания, что объяснятся наличием захваченных газовых пузырьков. Сравнение с ранее опубликованными работами показало, что полученные в них значения коэффициента теплопроводности твердого н-эйкозана являются более низкими, что является причиной расхождения между экспериментальными и численными результатами для фазового перехода в процессе затвердевания.